Optimization of variable speed limits at the freeway lane drop bottleneck

Chunbo Zhang[a,b,c*], Edward Chung[d], Nasser R. Sabar[e], Ashish Bhaskar[c], Yingfang Ma[f]

[a] *School of Traffic and Transportation, Shijiazhuang Tiedao University, Shijiazhuang 050043, China*

[b] *School of Transportation, Southeast University, Nanjing 211189, China*

[c] *Smart Transport Research Centre, Queensland University of Technology, Brisbane 4000, Australia*

[d] *Department of Electrical Engineering, Hong Kong Polytechnic University, Hong Kong, China*

[e] *Department of Computer Science and Information Technology, La Trobe University, Melbourne, Australia*

[f] *Hebei Provincial Communications Planning and Design Institute, Shijiazhuang, China*

*Corresponding author: zhangchunbochn@yeah.net

Optimization of Variable Speed Limits at the Freeway Lane Drop Bottleneck

The primary objectives of this study were to use variable speed limits (VSL) upstream of freeway lane drop to maintain capacity and reduce congestion. As driving behaviours are the main reasons leading to capacity drop and the microscopic simulation can reflect driving behaviours precisely, microscopic simulations were first used to test lane drop scenarios. The objective function and constraints determined according to traffic engineering practice were optimized using a modified genetic algorithm (GA) based on microscopic simulation to get the optimal speed limit combination. The modified GA can guarantee the solution diversity and optimal results. Then, the cell transmission model, a macroscopic flow model, was used to crosscheck the simulated results. Both microscopic and macroscopic analysis results demonstrated that VSL could only improve lane drop traffic efficiency if speed limits were set appropriately. This study provided a new process from microscopic to macroscopic aspects for analysing traffic problems.

Keywords: lane drop; capacity drop; variable speed limit; microscopic simulation; cell transmission model

1. Introduction

Due to road design, incident or road maintenance, lane drop or lane reduction is a common freeway bottleneck (Zhang et al. 2019). As vehicles approach a lane drop bottleneck, vehicles on the closed lane have to change lanes to get through the bottleneck. When traffic demand is high, the lane-changes of the closed lane are frequent. At the lane drop bottleneck, when the upstream is congested, the perturbation of frequent lane changes, bounded acceleration and so on leads to lower space mean speed and longer vehicle headways, and the maximum discharging flow-rate can drop to a level lower than the downstream capacity. It is the so-called “capacity drop”. The magnitude of the capacity drop is reported at around 10% in the literature (Cassidy and Rudjanakanoknad 2005; Jin and Jin 2015), and it varies under different traffic

conditions, such as with different acceleration spread, reaction time, lane changing behaviour and different percentages of heavy vehicles in the traffic stream (Yuan et al. 2017; Chamberlayne et al. 2012). The capacity drop at the bottleneck worsens the traffic condition, leading to an accelerated increase in congestion, with negative environmental and safety impacts. To avoid capacity drop, it is necessary to control upstream traffic and manage the traffic flow at the bottleneck. Srivastava and Geroliminis (2013) verified that the reasonable control strategy is expected to create smaller capacity drops than the no control case.

Control strategies of early merge (EM) and late merge (LM) are often used to improve lane drop traffic efficiency. The purpose of EM is to encourage drivers to switch to the open lane early, while for LM, vehicles in both open and closed lanes are advised to stay in their lanes respectively until the merge point, at which drivers take turns to merge (Ren et al. 2021). However, both EM and LM cannot eradicate the capacity drop phenomenon under high traffic demand. Other control strategies should be investigated to improve lane drop traffic efficiency. Variable speed limit (VSL) is widely used on urban streets and highways. VSL is usually used on urban streets to save fuel, reduce total delay and speed variance, decrease the number of stops and so on (Kamalanathsharma at al. 2015; Tajalli and Hajbabaie, 2018a; Tajalli and Hajbabaie, 2018b; Hao et al. 2019; Tajalli et al. 2020). For freeways, VSL is a traffic flow control strategy to protect the end of queue and maximize flow, has been a topic of research for over a decade (Hegyi et al. 2005; Han et al. 2017b; Grumert et al. 2015; Calson et al. 2010). Hadiuzzaman et al. (2013) developed the VSL based control strategy to maximize the flow at an active freeway bottleneck. The strategy was tested in a controlled environment using METANET, which is a second-order macroscopic flow model usually used for freeway sections. Chen et al. (2014) developed a theoretical

framework for VSL control, through analytical modelling, in which the key principle is to impose VSL control some distance upstream of a bottleneck to starve the inflow to the bottleneck and dissipate the queue. Once the queue near the bottleneck vanishes, another less restrictive VSL is imposed upstream to resolve the heavy queue generated by the first VSL and regulate the inflow to the bottleneck to sustain the stable maximum bottleneck discharge rate and prevent traffic breakdown. Chen and Ahn (2015) developed VSL schemes based on Kinematic Wave theory to increase discharge rates while smoothing speed transition at severe freeway lane drop bottlenecks induced by non-recurrent road events such as work zones or incidents. The main control principle is to restrict upstream demand progressively to achieve three objectives: (i) to provide gradual speed transition at the tail of an event-induced queue, (ii) to clear the queue around the bottleneck, and (iii) to discharge traffic at the stable maximum flow able to be sustained at the bottleneck without breakdown. For the traffic system in a zone upstream to a lane drop bottleneck, Jin and Jin (2014; 2015) based their formulation of the VSL control problem on two macroscopic traffic flow models: the Lighthill-Whitham-Richards (LWR) model and the link queue model. In both models, the discharging flow-rate was determined by a developed model of capacity drop, and the upstream in-flux was regulated by the speed limit in the VSL zone. Results indicated that VSLs based on integral (I) and proportional-integral (PI) controllers were stable, effective, and robust for the LWR model. Zhang and Ioannou (2015) developed a combined lane change and VSL control strategy that recommended lane changes in advance to relieve capacity drop. Microscopic Monte-Carlo simulations of traffic on a freeway with high truck demand were used to demonstrate that the combined control strategy was able to generate consistent improvements with respect to travel time, safety and environmental impact under different traffic conditions and incident scenarios. The

VSL controller was also developed using a feedback linearization approach based on the Cell Transmission Model (CTM) and was shown analytically to guarantee exponential convergence to the optimum equilibrium point (Zhang and Ioannou 2017). Muller et al. (2015) applied the local feedback mainstream traffic flow control with VSL in microscopic simulation for a bottleneck, and significant improvements in traffic conditions were obtained. Besides, Soriguera et al. (2017) used the real data on a freeway in Spain to analyse the low speed limit effects on traffic flow. It was confirmed that the lower the speed limit, the higher the occupancy to achieve a given flow, and VSL strategies are able to increase vehicle storage capacity of freeways under low speed limits.

These literatures have demonstrated benefits of VSLs for freeway performance. However, most of these studies were based on macroscopic traffic models, which cannot describe the driving behaviour leading to lane drop bottleneck congestion. Some researchers only used microscopic models or simulations to verify VSL effects, but not analyse the principle VSL law for capacity drop microcosmically. Capacity drop is the result of microscopic traffic behaviours. It is reasonable to analyse the speed limit effects based on microscopic traffic models, as microscopic models can describe traffic behaviours effectively. Then, the macroscopic should be used to verify the VSL effects from discharging flow, speed limit values, etc. Besides, only a few researchers (Hadiuzzaman et al. 2013; Hadiuzzaman and Qiu 2013) have optimized the VSL at the lane drop bottleneck, but they did not describe the optimization process clearly.

So this research aims to solve the problems below: a) Can the VSL be used to manage congestion at the freeway lane drop bottleneck? b) How to analyse VSL effects considering microscopic behaviours such as car-following and lane-changing behaviours through microscopic simulations and how to optimize the VSL based on

microscopic simulations to achieve optimal control at the lane drop section? c) How to crosscheck VSL results of microscopic simulations at lane drop section using macroscopic traffic flow models to guarantee the analysis accuracy?

The paper is organized as follows: the research problem from the microscopic perspective and VSL strategy is described in Section 2. The proposed optimization methodology based on microscopic simulations is introduced in Section 3. The microscopic simulation testing, the results and the crosscheck analysis based on the macroscopic model are presented in Section 4. Section 5 concludes the paper.

2. Problem description and variable speed limit strategy

From the microscopic perspective, the capacity drop mechanism of a lane drop is that vehicles on the closed lane (the leftmost lane in the paper as shown in Figure 1) will merge to the open lanes upstream of the bottleneck. Opportunities for lane changing differ in low and medium flows. When flow increases, lane changing becomes more difficult and acceptable gaps in the open lanes are fewer. The perturbation of lane changing during high flow, bounded acceleration and so on results in a drop in the capacity at the bottleneck. This capacity drop exacerbates the congestion, causing drops in speed and increases in the queue upstream of the bottleneck. From the macroscopic perspective, once the bottleneck density reaches the critical density, the bottleneck flow drops to a low level.

[Figure 1 near here]

Refer to Figure 1, the upstream of a three-to-two freeway lane drop section (left hand driving) is divided into n segments. Say the length of each segment is Δx for the VSL strategy: the aim is to determine the optimal speed limits for these n segments that minimize (or maximize) an objective under various constrains (e.g., related to traffic safety, acceptable maximum and minimum speed limit values) with known demand.

As analysed above, the capacity drop is because of microscopic traffic behaviours such as lane changes, acceleration, etc. It is reasonable to analyse the VSL effects to solve capacity drop problem firstly through microscopic models. This research adopted the widely used microscopic traffic simulation software AIMSUN (Rahman and Abdel-Aty 2021; Zhang et al. 2019; Zhou et al. 2019; Mai et al. 2016) including microscopic models, such as lane-changing models, car-following models, etc. AIMSUN can simulate the capacity drop phenomenon effectively, the API (Application Program Interface) function can input and output data conveniently, and the VSL control can be easily simulated in the AIMSUN and API environment. The relationship between AIMSUN and API is shown in Figure 2 (from AIMSUN API manual). For the current study, in order to make full use of freeway space-time resources and achieve VSL optimal control, we specify the objective to maximize the total throughput (which is a traffic efficiency indicator, equivalent to traffic flow if time is constant) not safety because micro-simulation is not a suitable tool for safety analysis or assessment. That is to minimize the inverse of the total throughput (Y) (as shown in Equation (1)) at the segment immediately downstream of the lane drop segment (downstream of segment 1 in Figure 1).

$$\min Y = 1/\left(\sum_{j=1}^{T/\Delta t} n_{throughput,j}\right) \quad (1)$$

where, T is the study period for which the VSL should be determined, Δt is the time interval for update of traffic conditions, $n_{throughput,\ j}$ denotes the vehicle volume into downstream during the j^{th} time interval which is derived through the microscopic simulation software AIMSUN based on microscopic traffic models for the current study.

[***Figure 2 near here***]

For the current study we specify the constraints based on Queensland, Australia practice except the low speed limit as follows:

- **C1: maximum speed constraint:** This is the maximum acceptable speed limit of the freeway section as shown in Equation (2).

$$v_i \leqslant v_{max}=100km/h,\ i=1,\ 2,\ \cdots,\ n \tag{2}$$

- **C2: deceleration constraint:** Here, considering the safety of the flow between the two segments, the drop in the speed limit between the upstream and the downstream consecutive segments is upper bounded by a threshold (Δv). Queensland Department of Transport and Main Roads recommends Δv as 20 km/h, as shown in Equation (3).

$$v_{i+1}-v_i \leqslant \Delta v = 20\ km/h,\ i=2,\ \ldots,\ n-1 \tag{3}$$

- **C3: speed limit value constraint:** If v_i is the minimum speed limit value in the speed limit combination, it can be any integer between *10* and *100* as shown in Equation (4). Otherwise, speed limit is rounded to the nearest 10 km/h as shown in Equation (5). The specific condition will be discussed in the Result Discussion Section.

$$v_i=10,11,12,13,\ldots,100km/h, \text{ if } v_i \text{ is the minimum speed limit value} \tag{4}$$

$$v_i=10,20,30,\ldots,100km/h, \text{ if } v_i \text{ is not the minimum speed limit value} \tag{5}$$

- **C5: the first upstream segment speed limit constraint:** For the analysis we consider the upstream-most segment (n^{th} segment) as the segment after which the VSL is applied. Therefore, the speed limit of the n^{th} segment is fixed to the maximum speed limit as shown in Equation (6).

$$v_n = v_{max} = 100km/h \quad (6)$$

3. Optimization methodology

In the previous section, we formulated VSLs as an optimization problem, where the optimal speed limits for each segment are determined through minimization of the objective function under various constraints. In order to present clear model formulation, the entire optimization model with the objective function and constraints is summarised in Figure 3.

[***Figure 3 near here***]

The VSL results are mainly analysed through the microscopic traffic simulation AIMSUN, so objective function values are calculated through microscopic car-following and lane-changing models in AIMSUN. There is no clear mathematical relationship between VSLs and the objective function. To this end, we resort to the genetic algorithm (GA) (Holland 1992) to effectively deal with VSLs. GA is a stochastic nature-inspired approach that has proven to effectively deal with various optimization problems. GA has been used to get VSL results through macroscopic models (Li et al. 2016; Yu and Fan 2019; Frejo et al. 2013; Frejo et al. 2014). A traditional GA often produces moderate solutions, but a high-quality solution can be achieved by customizing it to the problem at hand. Two modifications therefore have been made for GA to solve the VSL effectively. The flow charts of traditional GA and the proposed modified GA in this paper are shown in Figure 4 and Figure 5, respectively. Though the proposed modified GA cannot guarantee the global optimum, the preliminary tests indicated satisfied optimization results. In the subsections, detail of traditional GA and proposed modifications in GA are shown.

[***Figure 4 near here***]

[***Figure 5 near here***]

3.1 Traditional genetic algorithm

The genetic algorithm is a well-known stochastic nature-inspired approach (Holland 1992). Researchers have widely used it to solve hard optimization problems. GA consists of a set of individuals where each individual represents a solution to the problem at hand. The set of individuals form the population of solutions. The GA searching process is as follows: it first creates a population of solutions and then applies the so called evolutionary operators (selection, crossover and mutation) to evolve a new population of solutions. The new population will replace the old one if it has a better quality. This process will be repeated for a certain number of generations (iterations). The flowchart of GA (Tang et al. 2015) is shown in Figure 4 and its main steps are as follows:

- **Step 1:** *Set the parameters*: The GA parameters are initialized in this step. They are:
    - Maximum number of generations - indicates when GA search process will be halted.
    - Population size - indicates the number of solutions to form the population.
    - Crossover rate - represents the probability of applying crossover operator.
    - Mutation rate - represents the probability of applying mutation operator.
- **Step 2:** *Initialize a population of solutions*: In this step, each individual in the initial population is randomly initialized.
- **Step 3:** *Fitness calculation*: This step assigns a value for each individual indicating how good this individual compared to other ones.

- **Step 4:** *Selection*: The selection process forms the mating pool to be used by the crossover and mutation operators. It selects the participating individuals with probability proportional to their fitness values.
- **Step 5:** *Crossover*: The crossover operator attempts to evolve offspring solutions. It takes two solutions from the mating pool and then mixes their genetic materials.
- **Step 6:** *Mutation*: The mutation operator tries to help the search avoid the local optimal points. It randomly selects one or a few positions from a given solution and changes their values.
- **Step 7:** *Stopping condition*: This step is responsible for halting the search process. It checks the maximum number of generations and if this has been reached, the search will stop and return the best solution. Otherwise, it calculates the fitness values of the new solutions and replaces them with the old one if they are better.

3.2 Proposed modifications in GA

In order to use GA to deal with VSLs and to attain a high-quality solution, some modification should be made to customize the traditional GA effectively. The traditional GA faces two issues when dealing with VSLs. Firstly, the search process needs to ensure that all problem constraints are satisfied. Secondly, GA should be able to simultaneously accommodate the stochastic nature of the VSL and generate a high-quality solution. To address these issues, two modifications are proposed for a traditional GA. A repair procedure is utilized to ensure that the generated solutions do not violate the problem constraints. This is to guarantee that the search process did not go beyond the boundaries of the search space so it can focus on only feasible areas. To

deal with the stochastic nature of the VSL, a deletion-addition procedure is proposed to preserve the population diversity. This is to ensure that the population of the solutions is diverse enough and can capture the problem changes.

The flowchart of the proposed GA is shown in Figure 5. In this work, each solution is represented as a one-dimensional array with size equal to the number of segments, as shown in Table 1.

[*Table 1 near here*]

The main steps of the proposed GA are as follows:

- **Step 1:** *Set parameters:* Same as the traditional GA.
- **Step 2:** *Initialize a population of solutions*: The initial population will be processed to satisfy the constraints Equations (2-6).
- **Step 3:** *Fitness calculation*: Each individual of the population represents a VSL combination and is saved in a csv file. The csv file is read by API functions and inputted into the AIMSUN environment. During the simulation, the objective function of Equation (1) is calculated. After simulation, the result of objective function is outputted to another csv file. Then the fitness of each VSL combination is calculated. In this paper, the inverse of the objective function is the fitness function, because a better VSL combination should have a larger fitness value.
- **Step 4:** *Selection:* This section can be done in various ways. For instance, Roulette Wheel selection, Rank selection and Steady State selection (Boudissa and Bounekhla 2012; Bhunia et al. 2009). For the current analysis, we select Roulette Wheel selection to form the mating pool. The individual is selected according to the probability calculated in Equation (7).

$$P(i) = Fitness(i) / \sum_j Fitness(j) \quad (7)$$

- **Step 5:** *Crossover:* The crossover can be done in several ways, for example Single Point crossover, Two Point crossover, Uniform crossover and some others (Bao and Watanabe 2010). For this paper, we use a Two Point crossover operator, which works as follows: two points are randomly selected, the string from beginning of individual to the first crossover point is copied from one parent, the part from the first to the second crossover point is copied from the second parent and the rest is copied from the first parent, as shown in Figure 6.

[*Figure 6 near here*]

- **Step 6:** *Mutation:* The mutation operator tries to help the search avoid the local optimal points. It randomly selects one or a few positions from a given solution and changes their values within the search range, as shown in Figure 7.

[*Figure 7 near here*]

- **Step 7:** *Constraints handling:* The new individual generated by the crossover and mutation may not satisfy the constraints specified in Equations (2-6). The repairer procedure is executed to turn an infeasible solution into a feasible one, as shown in Equations (8-11). One example of the repairer procedure is shown in Figure 8 according to Equation (8) and Equation (9).

$$If\ (v_{i+1}-v_i)>20,\ then\ v_{i+1}=v_i+20\ (i=1,\ldots,\ n-1) \quad (8)$$

$$If\ v_n \neq v_{max},\ then\ v_n=v_{max} \quad (9)$$

$$If\ v_i>100,\ then\ v_i=100 (i=1,\ldots,\ n) \quad (10)$$

$$If\ v_i<10,\ then\ v_i=10 (i=1,\ldots,\ n) \quad (11)$$

[*Figure 8 near here*]

- **Step 8:** *Stopping condition:* Same as for traditional GA. It checks the maximum number of generations and if it has been reached, the search will stop and return the best solution. Otherwise, it calculates the fitness values of the new solutions and replaces them with the old one if they are better.
- **Step 9:** *Promoting diversity:* Our preliminary testing demonstrated that, after some generations, some individuals of the current population may be the same or very similar to each other. This can lead to the problem of premature convergence in which all individuals are located into the same area in the search space. To avoid this issue and promote diversity in the search process, some individuals are randomly deleted with high objective function values and added new individuals into the population to maintain the diversity of individuals.

4. Simulation settings and result discussion

4.1 Simulation settings

The optimization process is based on the microscopic traffic simulation software, AIMSUN. AIMSUN is an integrated transport modelling software, developed by Transport Simulation Systems (TSS). AIMSUN offers an API function that enables an interface with external applications so that users can apply their proposed strategies. The API function also enables script to be written to control the AIMSUN console application and is therefore very useful for batch simulation of many replications for a calibrated model. AUMSUN and API function have been used in many researches (Zhang et al. 2019; Mai et al. 2016; Zhou et al. 2019). The AIMSUN version used in

this study is 8.1.3.

This research took the three-to-two lane drop network as the research object. The three-to-two lane drop network is built in AIMSUN in the same way as shown in Figure 9. The model is calibrated using real data before optimization. This interactive process consists of changing model parameters and comparing model outputs with a set of real data to reflect the observed local traffic and driving behaviour conditions with speed limit 100 km/h being modelled (Mai et al. 2016). As analysed in previous research (Laval and Daganzo 2006), lane changes are the main cause of the dropped in the lane drop bottleneck discharging rate. Since lane changes lead to very slow vehicle speed, there will be some void in front of the lane changing vehicles and the acceleration rate will determine the discharging flow drop proportion. So the acceleration rate is an important parameter to be calibrated (Yuan et al. 2017). Gap and clearance in AIMSUN are also related to the discharging flow, and are selected as calibration parameters.

[***Figure 9 near here***]

The real data of discharging flow (from three-to-two lane drop) before and after the congestion on the M4 freeway near London, UK, shown in Table 2 (Bertini and Leal 2005), is compared with the output from AIMSUN. To get the discharging flow before and after congestion, the discharging flow of two normal lanes with enough high demand is regarded as the discharging flow before congestion at the three-to-two lane drop, and the discharging flow of three-to-two lane drop bottleneck when congestion occurs is regarded as the discharging flow after congestion. The default and calibrated values of parameters are shown in Table 3. The calibrated results of 20 replications, which have different random seeds, are shown in Table 4. Also, calibrated t-test results of the mean comparison between the outputs from AIMSUN and the real data of Day 1,

Day 2 and Day 3 in Table 2 are shown in Table 4. The validated t-test results of comparing 20 replications with the real data of Day 4 and Day 5 are also shown in Table 4. According to the t-values, the calibrated model is able to simulate observed traffic phenomenon well. In the research, only the case with speed limit 100km/h is calibrated. In fact, it is very difficult to precisely calibrate simulation models with different speed limits especially for very low speed limits. To a certain extent, the microscopic models included in AIMSUN can model various conditions with different speed limits. The models are used for further analysis.

[***Table 2 near here***]

[***Table 3 near here***]

[***Table 4 near here***]

4.2 Result discussion

Twenty replications of each speed limit combination were simulated using the optimization algorithm under three traffic demands: 4000 veh/h (higher than the discharging flow before congestion), 3600 veh/h (between discharging flows before and after congestion) and 3200 veh/h (below the discharging flow after congestion). The simulation time is 30 minutes, with the warm-up time of 10 minutes for each simulation; the base condition is the speed limit of 100 km/h on all segments upstream of the lane drop.

The results shown in Table 5 and Figure 10 showed that the optimized speed limit combination can improve the lane drop discharging flow. The flow increases from 3336 veh/h to 3616 veh/h, improving about 8.4% under the high traffic demand 4000 veh/h. A similar effect for medium traffic flow (3600 veh/h) can be obtained: the flow increases from 3356 veh/h to 3560 veh/h (6.1%). Besides, as the simulation is calibrated and validated with real data, the simulation's capacity is consistent with the real data of

near 3700 veh/h. Normally, the discharging flow with VSL is lower than or equals to capacity. The discharging flow from optimization method GA is 3616 veh/h under high traffic demand, which is, if not, very close to the real maximum discharging flow with optimal VSL. This further showed the effectiveness of the proposed approach in achieving maximum discharging flow.

[*Table 5 near here*]

[*Figure 10 near here*]

For the low traffic demand 3200 veh/h, the flow of optimized speed limit is almost the same as that for base case. No congestion occurs under both conditions as shown in Table 5, because the flow of either 3194 veh/h or 3198 veh/h is almost the same as the traffic demand 3200 veh/h. Hence when the traffic demand is lower than the discharging flow after congestion, there is no need to adopt the optimized speed limit combination: this is consistent with the confirmation of the VSL strategy is effective only if congestion occurs (Jin and Jin 2015).

Why the optimized speed limit combination in the upstream of lane drop can improve traffic efficiency is analysed below. If congestion occurs just before the lane drop bottleneck, the vehicles in the leftmost lane will make mandatory lane changes, which can lead to a void just before the lane changing vehicles and can also lead to low speed. A way to avoid the void and low speed at the bottleneck is through reducing flow into the bottleneck to reduce traffic density near bottleneck. If the traffic density is low, that is to say the space between vehicles are large, vehicles in the leftmost lane can make lane changes easily and the interference among vehicles will be small. Hence the traffic efficiency can be improved. Speed limit combination in the upstream of lane drop is used to reduce the flow into the bottleneck. The speed limit must be low enough to reduce the flow. However, the speed limit cannot be too low, as this will lead to a

lower discharging flow than that under congestion, which can be seen easily from Figure 11. Also, if the total travel time (TTT), which means total time spent (TTS) is used to represent the traffic efficiency, similar results can be obtained. In fact, the minimum speed limit value in the speed limit combination determines the overall lane drop network efficiency. If 10 km/h or 20 km/h is set as the minimum speed limit in the research, the traffic efficiency cannot be improved as shown in Figure 11 and it is why the minimum speed limit can be any integer between 10 and 100 as shown in Equation (4) about speed limit value constraint C3.

The traffic fundamental diagram can be well to explain the principle behind this. The flow and density scatter plot of the original Georgia State Route 400 (GA400) data, which was often used to calibrate traffic fundamental diagram (Zhang et al. 2017; Zhang et al. 2021), is shown in Figure 12. From Figure 12, though the scatters is widely distributed under high traffic density, it can be seen that the traffic fundamental diagram is near a triangle and slopes of lines from scatters to coordinate origin represent the corresponding speed. On the contrary, if different speed limits are set, the corresponding flow can be obtained, which is consistent with Highway Capacity Manual 2010 (HCM 2010). So the triangle traffic fundamental diagram is used for further analysis as shown in Figure 13. For the three-to-two lane drop, under the base condition, the minimum speed limit value of the speed limit combination is v and the maximum flow in the upstream is q_{max3}, which is bigger than the maximum flow q_{max2} in the downstream, so congestion will happen at the bottleneck. Then, the discharging flow will drop to q'_{max2}. If a big speed limit v_1 (for example *30 km/h* as shown in Figure 11) in Figure 13 is set as the minimum speed limit value in the upstream, the flow in the upstream is q_1, which is still bigger than q_{max2}. The lane drop location is still the active bottleneck, there is still congestion just near the lane drop location and capacity drop still occurs, so the speed

limit v_1 is not suitable here. If a low speed limit v_3 (for example *10 km/h* as shown in Figure 11) is used as the minimum speed limit value, the flow in the upstream is q_3, which is even smaller than the dropped discharging flow q'_{max2}. The segment with speed limit v_3 (Segment 2 as shown in Figure 10(b) is with the minimum speed limit value in the research) will be the active bottleneck, leading to more serious congestion. Segment 2 as shown in Figure 10(b) with small speed limit will move the active bottleneck from the lane drop location to segment 2. Only an ideal speed limit of v_2 (for example 13 km/h) between v_1 and v_3 can improve the traffic efficiency, allowing the flow into bottleneck of between q_{max2} and q'_{max2}, which will keep segment 2 as the active bottleneck and ensure that the traffic density is lower than the critical density of bottleneck. The proposed algorithm finds the optimal value of v_2 in this study. Theoretically, if the exact fundamental diagram is known, the best speed limit v_2 can be calculated through the geometric relationship.

[*Figure 11 near here*]

[*Figure 12 near here*]

[*Figure 13 near here*]

4.3 Crosscheck with cell transmission model

In order to crosscheck the validity of the results obtained from the above analysis from microscopic simulations, we test the VSL effects on the widely used macroscopic Cell Transmission Model (CTM). CTM was proposed by Daganzo (1994; 1995), can model flow-density-speed relationship clearly, and it does not focus on vehicle microscopic behaviours (e.g. acceleration and deceleration). CTM is widely used for VSL analysis (Zhang and Ioannou 2017; Han et al. 2017a). A network similar to that illustrated in Figure 9 is modelled in CTM. For CTM, the demand and supply must be provided before analysis. The triangular-shaped fundamental diagram is used here, and the

demand and supply functions (Hadiuzzaman and Qiu 2013) are shown in Figure 14. Figure 14(a) represents the demand and supply function of the cells downstream except the bottleneck cell; Figure 14(b) represents the cell upstream with speed limit; Figure 14(c) is a condition of the bottleneck cell, and the capacity drop proportion Δ is set if the cell density is equal to or more than the critical density. Parameters in CTM are shown in Table 6, where jam density is the inverse of the sum of vehicle length (4m, consistent with the default value in AIMSUN) and clearance (2.1m, consistent with the values in Table 3). Studies (Papageorgiou et al. 2008; Carlson et al. 2010) on backward wave speed using real data have shown that the backward wave speed will change slightly, but the amplitude is insignificant. In this study, we assume the backward wave speed as a constant value, which can be calculated according to the geometric relationship shown in Figure 15. The critical density under the speed limit can be calculated through Equation (12) according to the geometric relationship shown in Figure 15. Then, the values of all parameters needed in CTM are determined.

$$k_c' = \frac{v_{ff} \times k_j \times k_c}{v_{ff} \times k_c + v_{sl} \times (k_j - k_c)} \tag{12}$$

Where, k'_c denotes the critical density under speed limit v_{sl}, k_j denotes the jam density, and k_c is the critical density under free-flow speed v_{ff}.

[*Figure 14 near here*]

[*Figure 15 near here*]

[*Table 6 near here*]

If the condition with demand lower than the flow just before the congestion is simulated, the traffic density in bottleneck cell (Figure 14(c)) will always be less than the critical density and capacity drop phenomenon will never occur. There is no need to simulate the condition when the traffic demand is lower than the flow just before

congestion. Only traffic demand 4000 veh/h is simulated in CTM. The optimized speed limit combination obtained from AIMSUN, except the minimum value from microscopic simulation, is as the search domain, and the enumeration algorithm is used to determine the optimal speed limit combination. From Figure 16, it can be easily seen that the speed limit value 18km/h is the solution, and the optimal speed limit combination is shown in Figure 17. Though the optimal speed limit combination is not exactly the same as the result from the AIMSUN, the results are very similar. The shapes of flow vs. minimum speed limit in Figure 11 and Figure 16 are also very similar.

[*Figure 16 near here*]

[*Figure 17 near here*]

The traffic density, shown in Figure 18, can be seen to be lower under the optimal speed limit condition than that under the base condition. The optimal speed limit upstream of the lane can reduce the flow into the bottleneck and reduce the traffic density just before the bottleneck. This provides more space for vehicles to make lane changes easier. The analysis indicates that the optimal speed limit can reduce the lane drop bottleneck congestion and improve traffic efficiency. The macroscopic model CTM result is consistent with the microscopic traffic simulation result.

[*Figure 18 near here*]

Though the optimal speed limit combination reduces traffic congestion and improves traffic efficiency, there is a practical issue. The VSL can work well only if the minimum speed limit is low enough, even lower than 20 km/h. Soriguera et al. (2017) also confirmed that speed limit more than 40 km/h almost has no effects on traffic flow. However, such low speed limits are very difficult for drivers to comply with through variable message signs (VMS) on freeways. It can generate better benefits if connected and autonomous vehicles (CAV) are applied on freeways. CAVs can easily accelerate

or decelerate to comply with VSL of each segment through vehicle automatic control system according to corresponding vehicle position system (Wu et al. 2020a; Wu et al. 2020b; Yu and Fan 2019; Han et al. 2017b; Grumert and Tapani 2020; Ren et al. 2021). From the analysis above, in practice, if traffic demand is low (less than 3200 veh/h), the speed limit combination shown in Figure 19(a) is applied. If traffic demand is medium or high, the speed limit combination is smoothly transited from that shown in Figure 19(a) to Figure 19(b) except the speed limit value in segment 2. The multiple speed limits upstream of segment 2 are set to ensure safe deceleration and avoid rear accidents. The length from the upstream speed limit to segment 2 is about two kilometres, which is enough for vehicles to decelerate. For the segment 2 speed limit value, the microscopic and macroscopic analysis indicated it is slightly different, as shown in Figures 10(b) and 17. Actually, it is hard to determine the practical speed limit value from the theoretical aspect. In practice, the speed limit value in segment 2 can be easily obtained through half-interval search (Song et al., 2017) in the range from 10 km/h to 30 km/h in practical feedback control tests.

[*Figure 19 near here*]

5. Conclusion

This research systematically analysed the variable speed limit effects on lane drop traffic efficiency, based on microscopic traffic models through AIMSUN, with optimization of speed limit combination under constraints. The results indicated that VSLs reduce traffic congestion and improve traffic efficiency, which is consistent with the macroscopic model CTM results. The contributions of this study are as follows:

- As capacity drop is mainly caused by microscopic vehicle behaviours, the research analysed VSL effects on lane drop efficiency and the speed limits were

optimized based on micro-simulation using AIMSUN, which can simulate vehicle behaviours precisely.

- A macroscopic model CTM was used to crosscheck the results from microscopic simulation and it verified VSL effects. The process from microscopic to macroscopic analysis is more convincing, as capacity drop is mainly caused by microscopic behaviours and can lead to macroscopic phenomena, such as dropped discharging flow, low space mean speed, etc. It provides a new process for analysing traffic problems.
- The research found that the speed limit must be low enough, even lower than 20 km/h, to reduce the flow into lane drop bottleneck to reduce traffic density and provide more space for vehicles to make lane changes easily. However, according to traffic engineering practice, such low speed limit is difficult for drivers to comply with. If CAVs are applied on freeways, better benefits can be obtained.

As mentioned above, CAV is possible in future. More diverse VSL strategies with CAV at the lane drop bottleneck should be analysed including differential VSL control among lanes, VSL-lane changing (VSL-LC) control, and so on. These are the future work of these authors.

Acknowledgements

The first author was a visiting student (October 2016 to November 2017) at Smart Transport Research Centre at Queensland University of Technology sponsored by China Scholarship Council. Besides, the research was partially sponsored by the Science and Technology Research Project of Colleges and Universities in Hebei province of China (QN2020134).

Funding

This work was supported by the China Scholarship Council under Grant number 201606090148; and Science and Technology Research Project of Colleges and Universities in Hebei province of China under Grant number QN2020134.

Disclosure statement

No potential conflict of interest was reported by the author(s).

References

Bao, Z.G., and W. Takahiro. 2010. "Circuit Design Optimization Using Genetic Algorithm with Parameterized Uniform Crossover." *IEICE Transactions on Fundamentals of Electronics, Communications and Computer Sciences* 93 (1): 281-290. doi: 10.1587/TRANSFUN.E93.A.281.

Bertini, R.L., and M.T. Leal. 2005. "Empirical study of traffic features at a freeway lane drop." *Journal of Transportation Engineering* 131 (6): 397-407. doi: 10.1061/(ASCE)0733-947X(2005)131:6(397).

Bhunia, A.K., S. Kundu, T. Sannigrahi, and S.K. Goyal. 2009. "An Application of Tournament Genetic Algorithm in a Marketing Oriented Economic Production Lot-Size Model for Deteriorating Items." *International Journal of Production Economics* 119 (1): 112-121. doi: 10.1016/J.IJPE.2009.01.010.

Boudissa, E., and M. Bounekhla. 2012. "Genetic Algorithm with Dynamic Selection Based on Quadratic Ranking Applied to Induction Machine Parameters Estimation." *Electric Power Components and Systems* 40 (10): 1089-1104. doi: 10.1080/15325008.2012.682246.

Carlson, R.C., I. Papamichail, M. Papageorgiou, and A. Messmer. 2010. "Optimal Motorway Traffic Flow Control Involving Variable Speed Limits and Ramp Metering." *Transportation Science* 44 (2): 238-253. doi: 10.1287/TRSC.1090.0314.

Cassidy, M.J., and J. Rudjanakanoknad. 2005. "Increasing the Capacity of an Isolated Merge by Metering Its On-Ramp." *Transportation Research Part B-Methodological* 39 (10): 896-913. doi: 10.1016/J.TRB.2004.12.001.

Chamberlayne, E., H. Rakha, D. Bish. 2012. "Modelling the Capacity Drop Phenomenon at Freeway Bottlenecks Using the INTEGRATION Software." *Transportation Letters-The International Journal of Transportation Research* 4 (4): 227-242. doi: 10.3328/TL.2012.04.04.227-242.

Chen, D.J., S. Ahn, and A. Hegyi. 2014. "Variable Speed Limit Control for Steady and Oscillatory Queues at Fixed Freeway Bottlenecks." *Transportation Research Part B-Methodological* 70: 340-358. doi: 10.1016/J.TRB.2014.08.006.

Chen, D.J., and S. Ahn. 2015. "Variable Speed Limit Control for Severe Non-Recurrent Freeway Bottlenecks." *Transportation Research Part C-Emerging Technologies* 51: 210-230. doi: 10.1016/J.TRC.2014.10.015.

Daganzo, C.F. 1994. "The Cell Transmission Model: A Dynamic Representation of Highway Traffic Consistent with the Hydrodynamic Theory." *Transportation Research Part B-Methodological* 28 (4): 269-287. doi: 10.1016/0191-2615(94)90002-7.

Daganzo, C.F. 1995. "The Cell Transmission Model, Part II: Network Traffic." *Transportation Research Part B-Methodological* 29 (2): 79-93. doi: 10.1016/0191-2615(94)00022-R.

Frejo, J.R.D., A. Nunez, B.D. Schutter, and E.F. Camacho. 2013. "Model Predictive Control for Freeway Traffic Using Discrete Speed Limit Signals." *In 2013 European Control Conference (ECC)*: 4033–4038. doi: 10.1016/J.TRC.2014.06.005.

Frejo, J.R.D., A. Nunez, B.D. Schutter, and E.F. Camacho. 2014. "Hybrid Model Predictive Control For Freeway Traffic Using Discrete Speed Limit Signals." *Transportation Research Part C Emerging Technologies*, 46: 309-325. doi: 10.1016/j.trc.2014.06.005.

Grumert, E.F., and A. Tapani. 2020. "Bottleneck Mitigation through a Variable Speed Limit System Using Connected Vehicles." *Transportmetrica A: Transport Science* 16 (2): 213-233. doi: 10.1080/23249935.2018.1547332.

Grumert, E., X. Ma, and A. Tapani. 2015. "Analysis of a Cooperative Variable Speed Limit System Using Microscopic Traffic Simulation." *Transportation Research Part C-Emerging Technologies* 52: 173–186. doi: 10.1016/j.trc.2014.11.004.

Hadiuzzaman, M., T.Z. Qiu, and X.Y. Lu. 2013. "Variable Speed Limit Control Design for Relieving Congestion Caused by Active Bottlenecks." *Journal of Transportation Engineering-ASCE* 139 (4): 358-370. doi: 10.1061/(ASCE)TE.1943-5436.0000507.

Hadiuzzaman, M., and T.Z. Qiu. 2013. "Cell Transmission Model Based Variable Speed Limit Control for Freeways." *Canadian Journal of Civil Engineering* 40 (1): 46-56. doi: 10.1139/CJCE-2012-0101.

Han, Y., A. Hegyi, Y.F. Yuan, S. Hoogendoorn, M. Papageorgiou, and C. Roncoli. 2017a. "Resolving Freeway Jam Waves by Discrete First-Order Model-Based Predictive Control of Variable Speed

Limits." *Transportation Research Part C-Emerging Technologies* 77: 405 – 420. doi: 10.1016/j.trc.2017.02.009

Han, Y.J., D.J. Chen, and S. Ahn. 2017b. "Variable Speed Limit Control at Fixed Freeway Bottlenecks Using Connected Vehicles." *Transportation Research Part B-Methodological* 98: 113-134. doi: 10.1016/J.TRB.2016.12.013.

Hao, P., G.Y Wu, K. Boriboonsomsin, and M.J. Barth. 2019. "Eco-Approach and Departure (EAD) Application for Actuated Signals in Real-World Traffic." *IEEE Transactions on Intelligent Transportation Systems* 20 (1): 30–40. doi: 10.1109/TITS.2018.2794509.

Hegyi, A., B. De Schutter, and J. Hellendoorn. 2005. "Optimal Coordination of Variable Speed Limits to Suppress Shock Waves." *IEEE Transactions on Intelligent Transportation Systems* 6 (1): 102–112. doi: 10.1109/TITS.2004.842408.

Holland, J.H. 1992. *Adaptation in Natural and Artificial Systems: An Introductory Analysis with Applications to Biology, Control and Artificial Intelligence. Ann Arbor: University of Michigan Press.*

Jin, H.Y., and W.L. Jin. 2015. "Control of a Lane-Drop Bottleneck through Variable Speed Limits." *Transportation Research Part C-Emerging Technologies* 58: 568-584. doi: 10.1016/J.TRC.2014.08.024.

Jin, W.L., and H.Y. Jin. 2014. "Analysis and Design of a Variable Speed Limit Control System at a Freeway Lane-Drop Bottleneck: A Switched Systems Approach." In *53rd IEEE Conference on Decision and Control*, 1753-1758. doi: 10.1109/CDC.2014.7039652.

Kamalanathsharma, R.K., H.A. Rakha, and H. Yang. 2015. "Networkwide Impacts of Vehicle Ecospeed Control in the Vicinity of Traffic Signalized Intersections." *Transportation Research Record: Journal of the Transportation Research Board* 2503: 91–99. doi: 10.3141/2503-10.

Li, Z.B., P. Liu, C.C. Xu, and W. Wang. 2016. "Optimal Mainline Variable Speed Limit Control to Improve Safety on Large-Scale Freeway Segments." *Computer-Aided Civil and Infrastructure Engineering* 31 (5): 366–380. doi: 10.1111/mice.12164.

Laval, J.A., and C.F. Daganzo. 2006. "Lane-Changing in Traffic Streams." *Transportation Research Part B-Methodological* 40 (3): 251-264. doi: 10.1016/J.TRB.2005.04.003.

Mai, T., R. Jiang, and E.C.S. Chung. 2016. "A Cooperative Intelligent Transport Systems (C-ITS)-based Lane-changing Advisory for Weaving Sections." *Journal of Advanced Transportation* 50 (5): 752-768. doi: 10.1002/ATR.1373.

Muller, E.R., R.C. Carlson, W. Kraus, M. Papageorgiou. 2015. “Microsimulation Analysis of Practical Aspects of Traffic Control with Variable Speed Limits.” *IEEE Transactions on Intelligent Transportation Systems* 16 (1): 512-523. doi: 10.1109/TITS.2014.2374167.

Papageorgiou, M., E. Kosmatopoulos, and I. Papamichail. 2008. “Effects of Variable Speed Limits on Motorway Traffic Flow.” *Transportation Research Record: Journal of the Transportation Research Board* 2047: 37-48. doi: 10.3141/2047-05.

Rahman, H., and M. Abdel-Aty. 2021. “Application of Connected and Automated Vehicles in a Large-Scale Network by Considering Vehicle-to-Vehicle and Vehicle-to-Infrastructure Technology:” *Transportation Research Record: Journal of the Transportation Research Board* 2675 (1): 93-113. doi: 10.1177/0361198120963105.

Ren, T.Z., Y.C. Xie, and L.M. Jiang. 2021. “New England Merge: A Novel Cooperative Merge Control Method for Improving Highway Work Zone Mobility and Safety.” *Journal of Intelligent Transportation Systems* 25 (1): 107-121. doi: 10.1080/15472450.2020.1822747.

Song, L.H., X. Kang, and G.X. Mei. 2017. “Buoyancy Force on Shallow Foundations in Clayey Soil: An Experimental Investigation Based on the ‘Half Interval Search.’” *Ocean Engineering* 129: 637-641. doi: 10.1016/J.OCEANENG.2016.10.018.

Soriguera, F., I. Martínez, M. Sala, and M. Menéndez. 2017. “Effects of Low Speed Limits on Freeway Traffic Flow.” *Transportation Research Part C-Emerging Technologies* 77: 257-274. doi: 10.1016/J.TRC.2017.01.024.

Srivastava, A., and N. Geroliminis. 2013. “Empirical Observations of Capacity Drop in Freeway Merges with Ramp Control and Integration in a First-Order Model.” *Transportation Research Part C-Emerging Technologies* 30: 161–177. doi: 10.1016/J.TRC.2013.02.006.

Tajalli, M., and A. Hajbabaie. 2018a. “Distributed Optimization and Coordination Algorithms for Dynamic Speed Optimization of Connected and Autonomous Vehicles in Urban Street Networks.” *Transportation Research Part C-Emerging Technologies* 95: 497–515. doi: 10.1016/J.TRC.2018.07.012.

Tajalli, M., and A. Hajbabaie. 2018b. “Dynamic Speed Harmonization in Connected Urban Street Networks.” *Computer-Aided Civil and Infrastructure Engineering* 33 (6): 510–523. doi: 10.1111/MICE.12360.

Tajalli, M., M. Mehrabipour, and A. Hajbabaie. 2020. “Network-Level Coordinated Speed Optimization and Traffic Light Control for Connected and Automated Vehicles.” *IEEE Transactions on Intelligent Transportation Systems*, 1–12. doi: 10.1109/TITS.2020.2994468.

Tang, J., G. Zhang, Y. Wang , H. Wang, F. Liu. 2015. “A hybrid approach to integrate fuzzy C-means based imputation method with genetic algorithm for missing traffic volume data estimation.” *Transportation Research Part C: Emerging Technologies* 51: 29-40. doi: 10.1016/j.trc.2014.11.003.

Wu, W.J., R.C. Sun, A.N. Ni, Z.K. Liang, and H.F. Jia. 2020a. “Simulation and Evaluation of Speed and Lane-Changing Advisory of CAVS at Work Zones in Heterogeneous Traffic Flow.” *International Journal of Modern Physics B* 34 (21): 2050201. doi: 10.1142/S021797922050201X.

Wu, Y.K., H.C. Tan, L.Q. Qin, and B. Ran. 2020b. “Differential Variable Speed Limits Control for Freeway Recurrent Bottlenecks via Deep Actor-Critic Algorithm.” *Transportation Research Part C-Emerging Technologies* 117: 102649. doi: 10.1016/J.TRC.2020.102649.

Yuan, K., V.L. Knoop, and S.P. Hoogendoorn. 2017. “A Microscopic Investigation into the Capacity Drop: Impacts of Longitudinal Behavior on the Queue Discharge Rate.” *Transportation Science* 51 (3): 852-862. doi: 10.1287/TRSC.2017.0745.

Yu, M., and W.D. Fan. 2019. “Optimal Variable Speed Limit Control in Connected Autonomous Vehicle Environment for Relieving Freeway Congestion.” *Journal of Transportation Engineering, Part A: Systems* 145 (4): 4019007. doi: 10.1061/JTEPBS.0000227.

Zhang, C.B., X.C. Guo, and Z.P. Xi. 2017. “Determination of Observation Weight to Calibrate Freeway Traffic Fundamental Diagram Using Weighted Least Square Method (WLSM).” *Promet-Traffic & Transportation* 29 (2): 203-212. doi: 10.7307/PTT.V29I2.2088.

Zhang, C.B., Z.G. Huang, and Y.G. Wang. 2021. “A Traffic Fundamental Diagram Calibrating Methodology to Avoid Unbalanced Speed-Density Observations.” *Transport* 36 (1): 13–24. doi: 10.3846/TRANSPORT.2021.14302.

Zhang, C.B., N.R. Sabar, E. Chung, A. Bhaskar, and X.C. Guo. 2019. “Optimisation of Lane-Changing Advisory at the Motorway Lane Drop Bottleneck.” *Transportation Research Part C-Emerging Technologies* 106: 303-316. doi: 10.1016/J.TRC.2019.07.016.

Zhang, Y., and P.A. Ioannou. 2015. “Combined variable speed limit and lane change control for truck-dominant highway segment.” In: *2015 IEEE 18th International Conference on Intelligent Transportation Systems*, 1163-1168. doi: 10.1109/ITSC.2015.192.

Zhang, Y.H., and P.A. Ioannou. 2017. “Combined Variable Speed Limit and Lane Change Control for Highway Traffic.” *IEEE Transactions on Intelligent Transportation Systems* 18 (7): 1812-1823. doi: 10.1109/TITS.2016.2616493.

Zhou, Y., E. Chung, A. Bhaskar, and M.E. Cholette. 2019. “A State-Constrained Optimal Control Based Trajectory Planning Strategy for Cooperative Freeway Mainline Facilitating and on-Ramp Merging Maneuvers under Congested Traffic.” *Transportation Research Part C-Emerging Technologies* 109: 321-342. doi: 10.1016/J.TRC.2019.10.017.

Tables with captions

Table 1 GA solution representation for VSL-combination of speed limits for n segments

Segment 1	*Segment 2*	*Segment 3*	*…*	*…*	*Segment n-1*	*Segment n*
80 km/h	60 km/h	40 km/h	…	...	90 km/h	100 km/h

Table 2 Lane drop discharging flow before and after congestion on M4

Day	Discharging flow before congestion		Discharging flow after congestion		Drop percent (%)
	Rate (vehicles/h)	Duration (h:min:s)	Rate (vehicles/h)	Duration (h:min:s)	
Day1	3690	0:17:50	3300	2:22:06	10.6
Day2	3690	0:14:45	3300	2:19:25	10.6
Day3	3750	0:11:57	3500	1:33:32	6.7
Day4	3840	0:08:07	3430	2:06:09	10.7
Day5	3510	0:13:12	3150	4:52:22	10.3
Mean	3700	--	3340	--	9.7

Table 3 Default and calibrated values of parameters in AIMSUN

	Default values			
	Mean	Deviation	Minimum	Maximum
Clearance	1.00 m	0.30 m	0.50 m	1.50 m
Max Acceleration	3.00 m/s^2	0.20 m/s^2	2.60 m/s^2	3.40 m/s^2
Gap	0.00 secs	0.00 secs	0.00 secs	0.00 secs
	Calibrated values			
	Mean	Deviation	Minimum	Maximum
Clearance	2.10 m	0.30 m	1.60 m	2.60 m
Max Acceleration	2.20 m/s^2	0.20 m/s^2	1.80 m/s^2	2.60 m/s^2
Gap	1.80 secs	0.10 secs	1.60 secs	2.00 secs

* Only passenger car is considered in this study; other vehicle types are not included, such as trucks.

Table 4 Discharging flow with default and calibrated parameter values

	Results with default parameter values				
	Replications	Mean (veh/h)	Standard deviation	[95% confidence interval]	t-value
Discharging flow before congestion	20	4845.3	25.66	[4833.3 4857.3]	54.6***
Discharging flow after congestion	20	4143.0	40.50	[4124.0 4162.0]	11.5**
	Results with calibrated parameter values				
	Replications	Mean (veh/h)	Standard deviation	[95% confidence interval]	Calibrated t-value (Validated t-value)
Discharging flow before congestion	20	3717.1	27.37	[3704.3 3729.9]	0.3(0.3)
Discharging flow after congestion	20	3344.7	21.48	[3334.6 3354.8]	-0.3(0.4)

*, ** and *** denote significant level 0.05, 0.01 and 0.001, respectively.

Table 5 Optimization results under different traffic demand

Traffic demand (veh/h)	Speed limit combination from upstream of the lane drop location (The base speed limit condition)	Flow (veh/h) (The base speed limit condition)
4000	**Figure 10(b)** (**Figure 10(a)**)	3616 (3336)
3600	**Figure 10(c))** (**Figure 10(a)**)	3560 (3356)
3200	**Figure 10(d)** (**Figure 10(a)**)	3198 (3194)

Table 6 Parameter values in CTM

Parameters	Values	Parameters	Values
Length of each cell	300 m	Critical density under free-flow speed	1850/100=18.5 veh/km/ln
Free flow speed	100 km/h	Backward wave speed (w)	1850/(164-18.5)=12.7 km/h
Simulation time step	300/(100/3.6)=10.8 secs	Critical density under speed limit	Equation(12)
Jam density	1000/(4+2.1)=164 veh/km/ln	Flow drop proportion	9.7%
Maximum flow of each lane	3700/2=1850 veh/h		

Figures

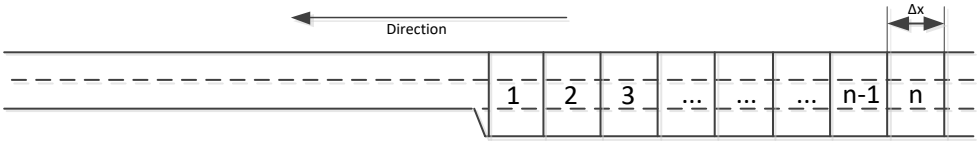

Figure 1 Freeway lane drop section (left hand driving)

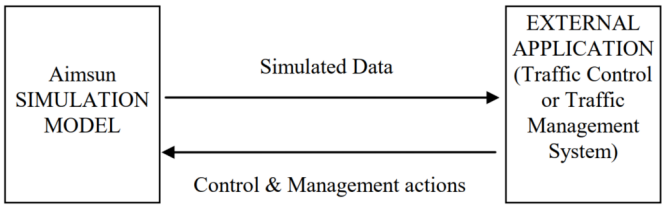

(a) AIMSUN environment without API function

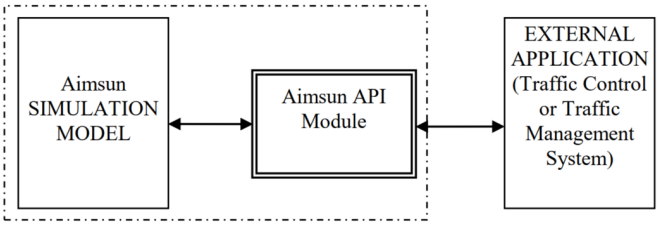

(b) AIMSUN environment with API function

Figure 2 AIMSUN and API relationship

Objective function $\min Y = 1/\left(\sum_{j=1}^{T/\Delta t} n_{throughput,j}\right)$

Constraints

- $v_i \leqslant v_{max}=100km/h,\ i=1,\ 2,\ \cdots,\ n$
- $v_{i+1}-v_i \leqslant \Delta v = 20\ km/h,\ i=2,\ \ldots,\ n-1$
- $v_i=10,11,12,13,\ldots,100km/h$, if v_i is the minimum speed limit value
- $v_i=10,20,30,\ldots,100km/h$, if v_i is not the minimum speed limit value
- $v_n=v_{max}=100km/h$

Figure 3 The entire optimization model with objective function and constraints

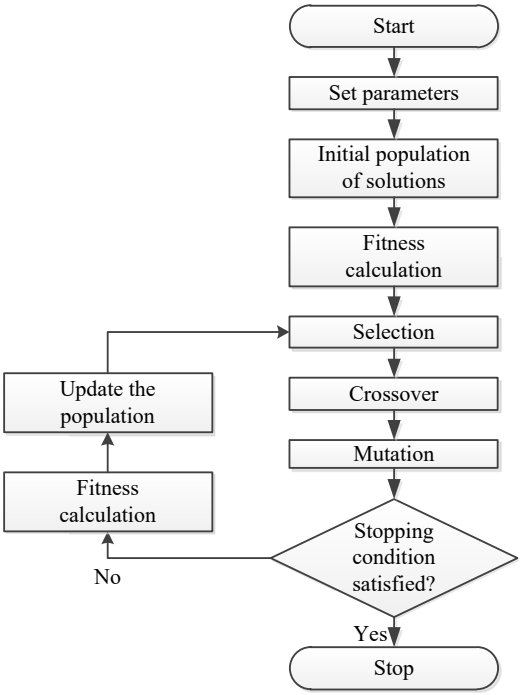

Figure 4 Traditional GA flowchart

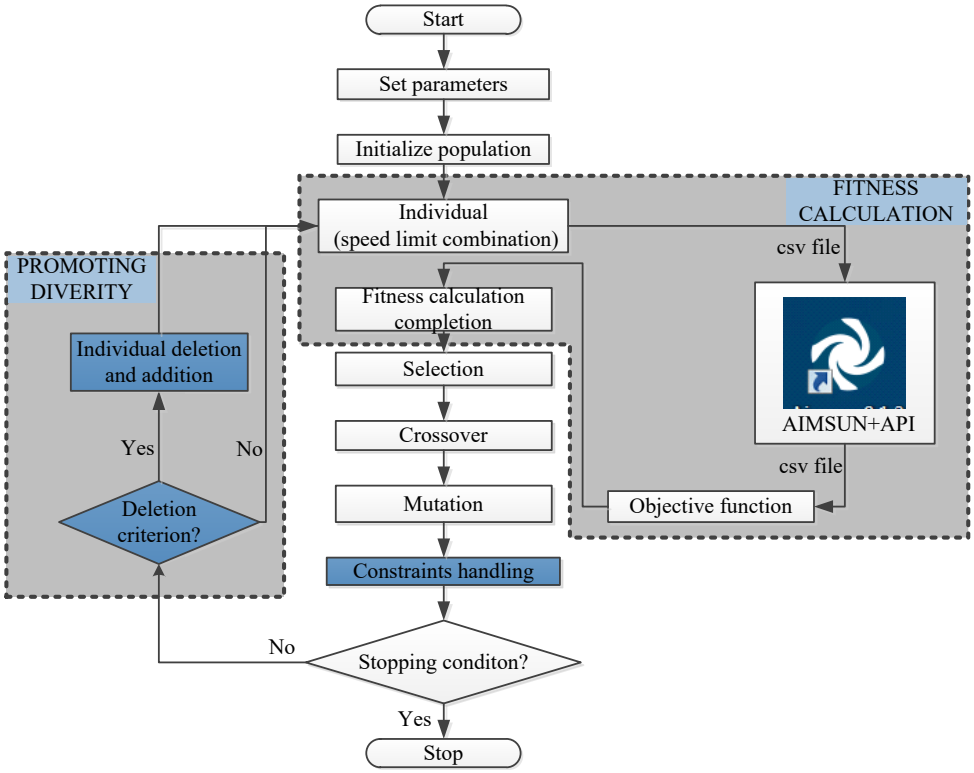

Figure 5 The proposed GA flowchart

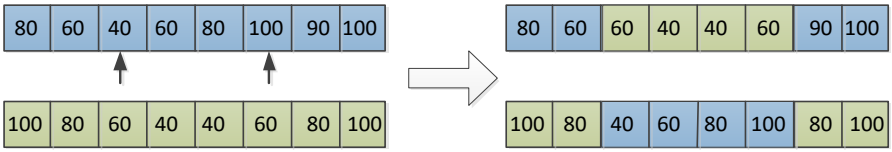

Figure 6 Two crossover points' operator

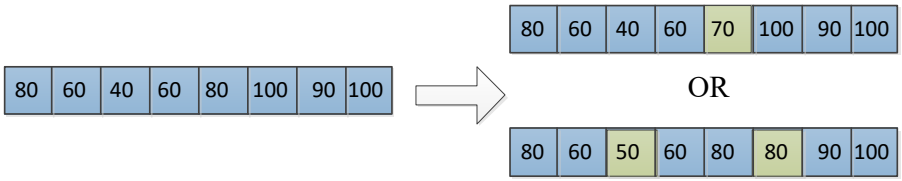

Figure 7 The mutation operator

Figure 8 The repairer procedure

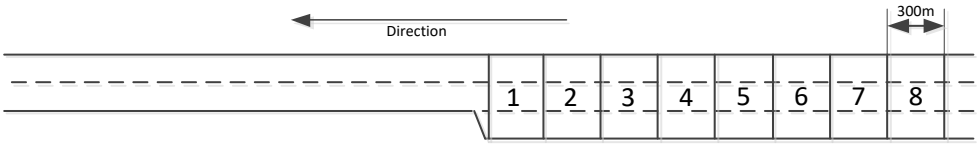

Figure 9 The AIMSUN lane drop model

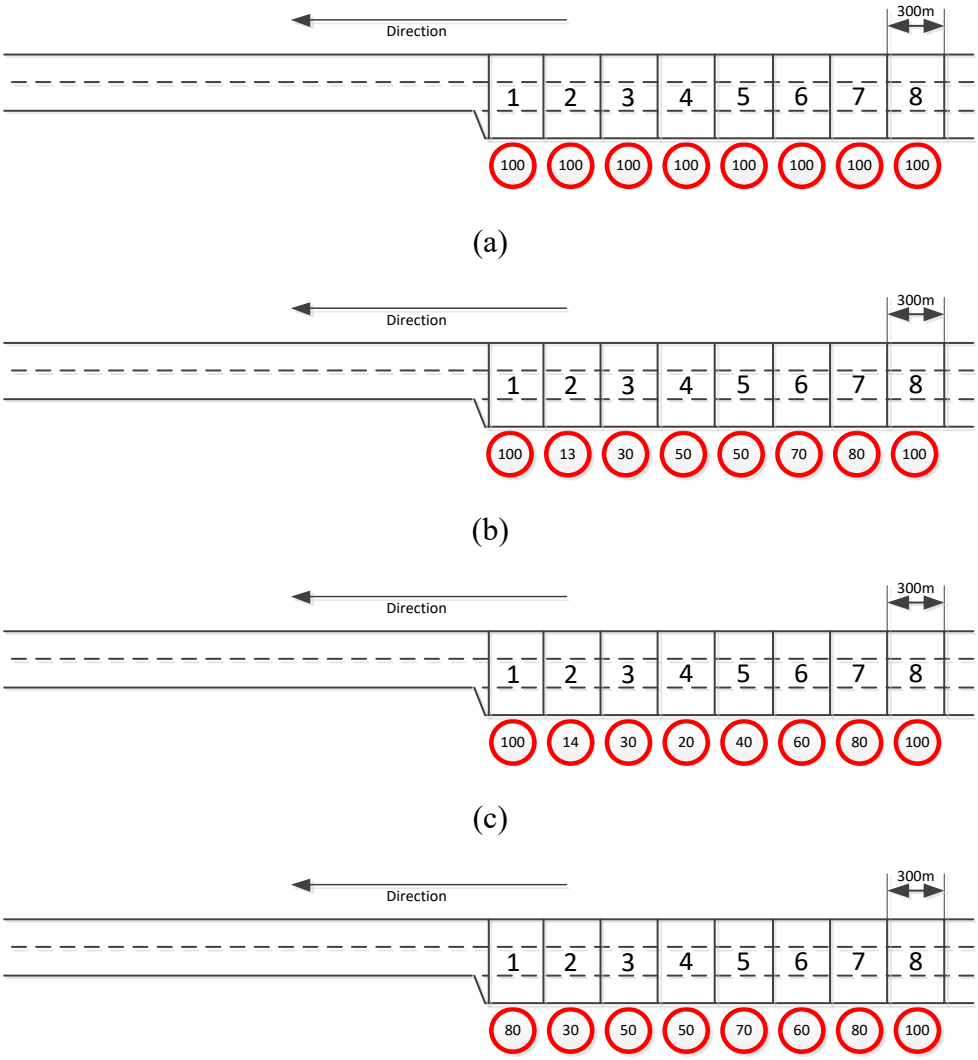

Figure 10 Speed limit combinations under different conditions: (a) base speed limit, (b) optimized speed limit under traffic demand 4000 veh/h, (c) optimized speed limit under traffic demand 3600 veh/h, and (d) optimized speed limit under traffic demand 3200 veh/h

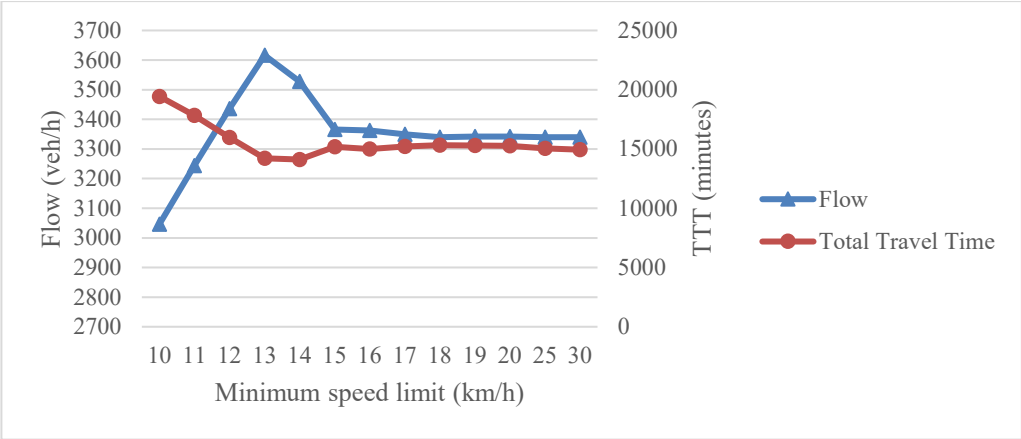

Figure 11 Flow and total travel time with different minimum speed limits with demand 4000 veh/h

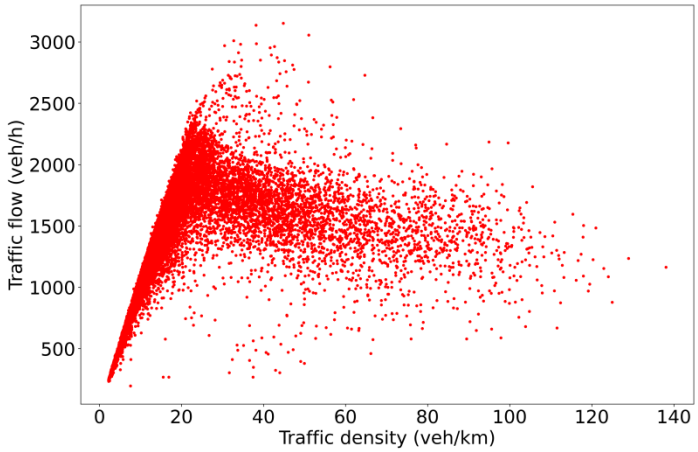

Figure 12 Flow and density scatter plot of the original GA400 data

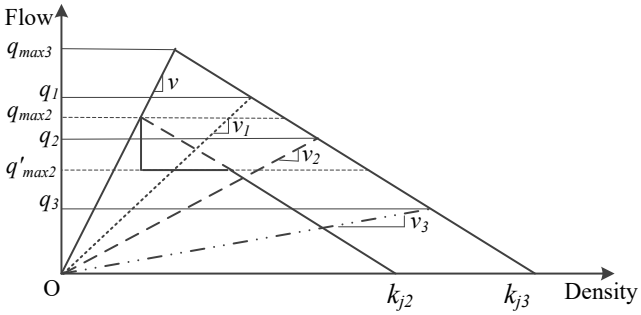

Figure 13 Fundamental diagrams under different speed limits

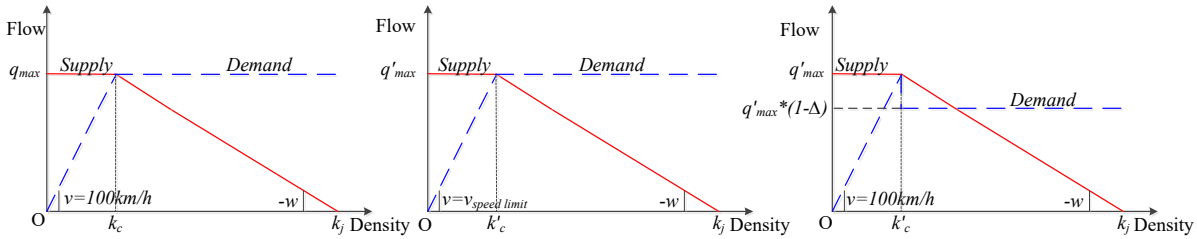

Figure 14 The cell demand and supply in CTM, (a) demand and supply function of the cells downstream except the bottleneck cell; (b) demand and supply function of the cell upstream with speed limit; (c) demand and supply function of the bottleneck

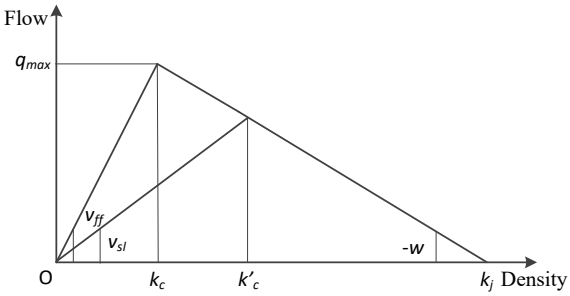

Figure 15 Geometric relationships between speed limit and critical density

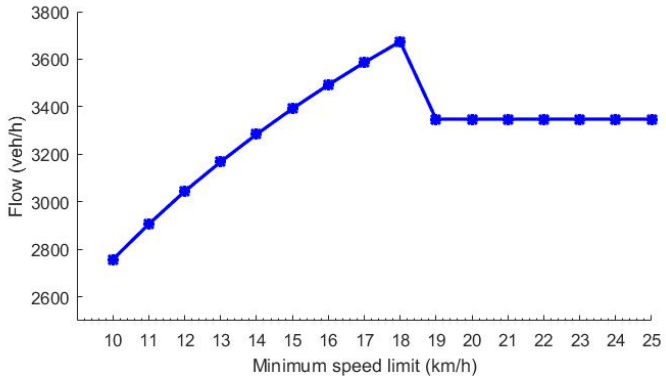

Figure 16 The flow under different minimum speed limits

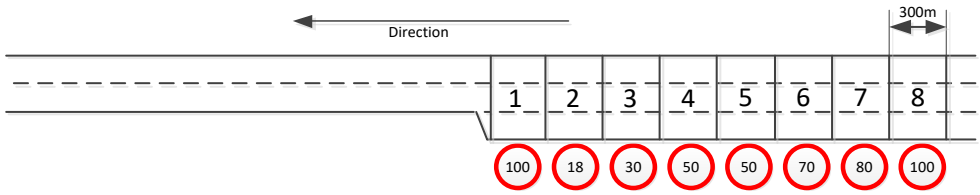

Figure 17 Optimal speed limit combination from CTM

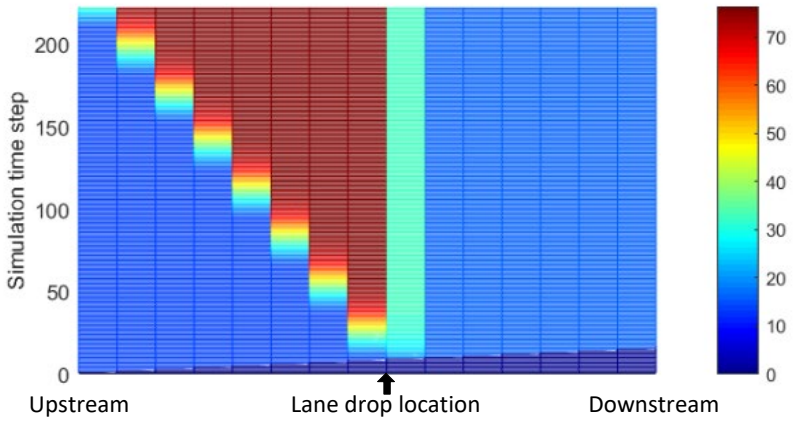

(a)

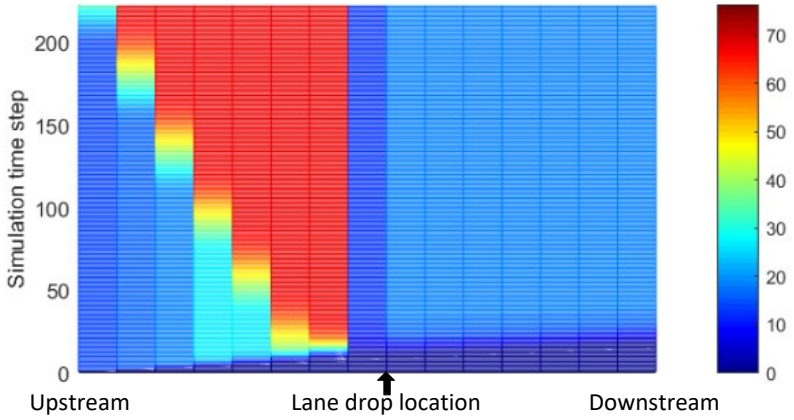

(b)

Figure 18 Traffic density (veh/km) under (a) base speed limit condition, (b) optimal speed limit condition

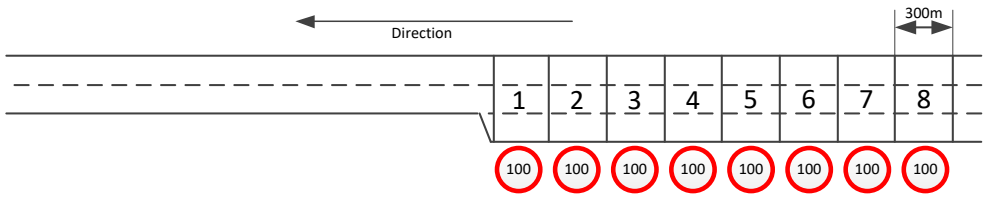

(a)

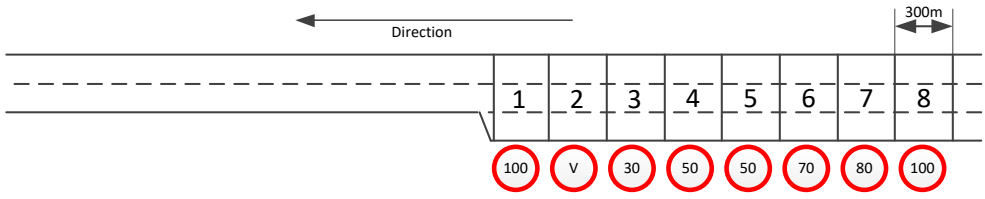

(b)

Figure 19 Speed limit combinations in practice (a) for low traffic demand, (b) for medium and high demand

Figure captions (as a list)